Pflugers Arch - Eur J Physiol (2004) 447: 392–400
DOI 10.1007/s00424-003-1204-y

Han-Gang Yu · Zhongju Lu · Zongming Pan · Ira S. Cohen

Tyrosine kinase inhibition differentially regulates heterologously expressed HCN channels

Received: 4 September 2003 / Revised: 10 October 2003 / Accepted: 15 October 2003 / Published online: 21 November 2003

Abstract The HCN ion channel subunit gene family encodes hyperpolarization-activated cation channels that are permeable to Na^+ and K^+. There are four members of this channel family, three of which, HCN1, HCN2, and HCN4, are expressed in the heart. Current evidence suggests that the HCN ion channel subunit family is the molecular correlate of the alpha subunit of the cardiac pacemaker current i_f. Our previous work has shown that HCN4 is the dominant isoform expressed in the rabbit sinoatrial (SA) node and that changes in tyrosine phosphorylation, either by kinase inhibition or growth factor activation, lead to changes in rabbit SA node i_f conductance with no change in voltage dependence. In the present study we investigate the actions of genistein, a tyrosine kinase inhibitor, on heterologously expressed HCN currents in *Xenopus* oocytes. Genistein had no effect on HCN1-induced currents, but reduced whole-cell currents induced by HCN2 or HCN4 and slowed activation kinetics at voltages near the midpoint of activation. In the case of HCN2 there was also a negative shift in the voltage dependence of activation that accompanies the current reduction. We have shown previously that HCN2 is the dominant isoform expressed in rat ventricular myocytes. The above results predict that genistein should reduce i_f in the rat ventricle and cause a negative shift of voltage dependence and kinetics of activation. We tested this hypothesis by studying the effects of genistein on isolated rat ventricular myocytes. Genistein significantly reduced i_f current density (pA/pF) (control: 12.2±1.8; genistein: 3.5 ±0.5; washout: 7.7±0.8; n=10), and caused a negative shift of the midpoint of activation by 14 mV (−133±1 mV for genistein and −119±1 mV for washout, n=7) with no change in slope factor. Our results thus suggest that i_f in the heart and i_f-like currents in other tissues can be regulated differentially by tyrosine phosphorylation based on isoform expression patterns.

Keywords i_f · HCN channels · Tyrosine phosphorylation · Genistein · Rat ventricular myocytes

H.-G. Yu (✉)
New York College of Osteopathic Medicine of New York Institute of Technology,
New York, N.Y., USA
e-mail: hgyu@nyit.edu
Tel.: +1-516-6863811
Fax: +1-516-6863832

Z. Lu · Z. Pan · I. S. Cohen
Institute of Molecular Cardiology and Department of Physiology and Biophysics, SUNY at Stony Brook,
Stony Brook, N.Y., USA

Introduction

Phosphorylation is an important regulatory mechanism governing many cell activities. Ion channels are no exceptions, since the gating and ion permeation of calcium channels, sodium channels and potassium channels have been reported to change with phosphorylation state [3]. Although the majority of previous studies have focused on serine-threonine kinases, a growing body of literature also has demonstrated important effects on ion channels mediated through changes in tyrosine phosphorylation state [3]. Our own previous work on the cardiac pacemaker current, i_f, (f for "funny", since the current is activated by hyperpolarization, as opposed to most ionic currents activated by depolarization) has demonstrated that sinoatrial (SA) node i_f is reduced by inhibition of tyrosine kinase activity by genistein or herbimycin A and enhanced by its stimulation with epidermal growth factor (EGF), which also increases heart rate [12, 13, 16, 17].

Within the last 5 years a family of four genes encoding the hyperpolarization-activated, cyclic nucleotide-gated cation channels (HCN) have been cloned and expressed in heterologous expression systems [5, 10, 11, 14]. Three members of this channel family are expressed non-uniformly in cardiac tissues [15]: abundant HCN4 and low levels of HCN2 transcripts are expressed in the SA node whilst, in contrast, much higher levels of HCN2 than HCN4 transcripts are present in the ventricle. HCN1 transcripts are expressed at low levels in the SA node and largely absent in ventricle. This differential expression

raises the possibility that pacemaker activity in one cardiac region could be altered without the necessity of changing it in another. Because of the wide distribution of these HCN ion channel subunits in non-cardiac tissue types, specific drug actions on selected family members might avoid potential wide-ranging drug side-effects.

Given the availability of the cloned family members for heterologous expression and the potential advantages of a selective pharmacology, we decided to investigate the actions of tyrosine kinase inhibition on each of the HCN channel subunits expressed in cardiac tissues. We tested this hypothesis further by investigating the effects of genistein on i_f in rat ventricular myocytes. Our results support the hypothesis that HCN channel subunits and regional cardiac i_f can be regulated differentially by tyrosine phosphorylation.

Materials and methods

Isolation of rat ventricular myocytes

Male Wistar rats weighing 175–200 g were heparinized by tail vein injection and then euthanized by decapitation following anesthesia using an isofluorane drip. All protocols were approved by the Institutional Animal Care and Use Committee. The heart was removed, placed in Tyrode's solution containing (in mM): NaCl, 137; $MgCl_2$, 0.5; glucose, 10; KCl, 5.4; $CaCl_2$, 1.8; and HEPES-NaOH, 11.8 (pH adjusted to 7.4 with NaOH), and squeezed gently to expel the blood. Ventricular myocytes were prepared using a Langendorff perfusion apparatus. Briefly, the hearts were removed and perfused with calcium-free Tyrode's containing (in mM): NaCl, 130; $MgSO_4$, 1.2; KCl, 5.4; KH_2PO_4, 1.2; HEPES-NaOH, 6 (pH adjusted to 7.2 with NaOH) with collagenase (Liberase Blendzyme 4, 0.1 mg/ml, Roche Molecular Biochemicals) for approximately 9 min. After washing out the collagenase with calcium-free Tyrode's, single cells were dissociated by mincing the ventricle and shaking the tissue in "Kraftbrühe" (KB) solution containing (in mM): KCl, 83; K_2HPO_4, 30; $MgSO_4$, 5; Na-pyruvate, 5; Na-β-hydroxybutyrate, 5; creatine, 5; taurine, 20; glucose, 10; EGTA, 0.5; HEPES-KOH, 5; ATP-Na_2, 5 (pH adjusted to 7.2 with KOH). Cells were washed and resuspended in KB.

Patch-clamp recordings of ventricular i_f

The isolated rat ventricular cells were placed in a Lucite bath maintained at 35±1°C. i_f was recorded using the whole-cell patch-clamp technique and an appropriate amplifier (Axopatch-1B, Axon Instruments, Foster City, Calif., USA). Pipette resistance was 1–3 MΩ when filled with solution containing (in mM): K-aspartate, 80; KCl, 50; $MgCl_2$, 1; EGTA, 10; Mg-ATP, 3; HEPES, 10 (pH adjusted to 7.2 with KOH). The external solution contained (in mM): NaCl, 90; NaOH, 2.3; $MgCl_2$, 1; KCl 50; $CaCl_2$, 1.8; $MnCl_2$, 2; HEPES, 5; glucose, 10; $CdCl_2$ 1; $BaCl_2$, 30; (pH adjusted to 7.4 with NaOH). The elevated K^+ was used to enhance i_f amplitude, Mn^{2+} and Cd^{2+} were employed to reduce Ca^{2+} currents, which can obscure i_f tail currents, and Ba^{2+} was used to block i_{K1} that activates and inactivates in the same voltage range as i_f.

The data were acquired by Clampex software (pClamp v. 8, Axon) and analyzed by Clampfit (pClamp 8, Axon). Because the amplitude of i_f was smaller in the presence of genistein and activated at more negative potentials, there was some initial overlap with Ba^{2+} blockade of i_{K1}. We therefore fitted i_f with a single exponential function starting 1 s after the onset of the hyperpolarizing voltage step until its conclusion ("i_f steady state"). We then extrapolated the fit back to the start of voltage step ("i_f initial"). The amplitude of i_f was the difference between i_f initial and i_f steady state. On washout the activation was more positive and i_f current amplitude much larger. In this case the entire i_f decay was fit to a single exponential and the i_f amplitude was considered the difference between the initial and final, steady-state values of the fit to the i_f decay. The activation threshold of i_f was defined as the least negative voltage at which a time-dependent current of at least 10 pA was observed (a value that allowed clear discrimination from background noise). Currents were normalized to cell membrane capacitance. Data were low-pass filtered with a cut-off of 20–30 Hz and are shown as means ±SEM.

Heterologous expression in *Xenopus* oocytes

Oocytes were prepared from mature female *Xenopus laevis* in accordance with an approved protocol as previously described [18]. Oocytes were injected with 5 ng cRNA made from mouse HCN1 and HCN2 and human HCN4 cDNA plasmids. Complementary RNA for HCN1 and HCN2 were made by linearizing pSD64TF vector using *Sph* I for HCN1 and pGHE vector using *Xba* I. cRNA for HCN4 was made by linearizing pcDNA1.1/Amp vector using *Xba* I. Injected oocytes were incubated at 18°C for 24–48 h prior to electrophysiological analysis.

For electrophysiological studies, oocytes were voltage-clamped using a two-microelectrode voltage-clamp technique. The holding potential was −30 mV. The extracellular recording solution (OR2) contained (in mM): 80 NaCl, 2 KCl, 1 $MgCl_2$, and 5 Na-HEPES (pH adjusted to 7.6 with NaOH). The steady-state activation curves were constructed from tail currents recorded at 0 mV in response to 2-s (for HCN1) or 7.5-s (for HCN2 and HCN4) hyperpolarizing test pulses unless otherwise stated. The waiting time between test pulses at different potentials (e.g., −55 mV, −65 mV) was 20 s for HCN1 and 50 s for HCN2 and HCN4. Because HCN2 and HCN4 activate slowly near the midpoint of activation, the 7.5-s pulse is not long enough to activate the current fully. The current traces were therefore fitted beyond the duration of the pulse to 20 s using a single exponential function to obtain the fully activated current amplitude. In the presence of genistein, HCN4 currents were fitted for 40 s to reach steady state. The ratios of current amplitudes at the end of the 20-s (for HCN2) and 40-s (HCN4) periods over that at the end of the 7.5-s period were multiplied to the corresponding tails to obtain the fully activated values. The maximal whole-cell conductance was calculated by taking the largest tail current (corresponding to the most negative test pulse) and dividing it by the driving force (difference between the test voltage and the reversal potential which was measured in each oocyte).

Group data are presented as means±SEM. The significance of differences between means of midpoint and slopes of activation curves was established using unpaired *t*-tests. $P<0.05$ was considered significant. Genistein and daidzein were purchased from LC labs (Woburn, Mass., USA). Stock solutions (100 mM) were made using DMSO. A final concentration of 0.1 mM was used in the experiments. DMSO content in the perfusion solution is 0.1%, which itself did not affect the expressed HCN currents.

Results

Tyrosine kinase inhibition does not alter HCN1-induced membrane currents

We employed genistein, a membrane-permeant inhibitor of tyrosine kinases, to investigate the role of basal tyrosine phosphorylation on HCN1-induced membrane currents in *Xenopus* oocytes. Our protocol was aimed at examining the activation curve and the kinetics of activation. Figure 1 (inset) shows a schematic of our voltage-clamp protocol.

From a holding potential of −30 mV, the membrane was hyperpolarized for 2 s to potentials between −65 mV and −125 mV in −10-mV increments and then stepped to 0 mV for 1.5 s to record the tail currents, after which it was stepped back to the holding potential. In Fig. 1 sample membrane currents in control, prior to application of genistein (Fig. 1A), after a 5- to 15-min exposure to genistein (Fig. 1B), and after washout of genistein (Fig. 1C) are shown. In Fig. 1D the currents in response to the step to −85 mV in the control and in the presence of genistein are plotted together. They superimpose, suggesting little or no effect of genistein on HCN1-induced currents.

The effects of genistein on HCN1 gating are shown in Fig. 1E and F. The activation curves for the control and genistein of this data set are plotted in Fig. 1E. The data were fitted to the Boltzmann two-state equation: $1/\{1+\exp[(V_{1/2}-V_{test})/s]\}$, where $V_{1/2}$ is the activation midpoint and s the slope factor. The values of $V_{1/2}$ and s were −82 mV and 8.6 mV in control and −82 mV and 7.8 mV with genistein, respectively. The corresponding means (n=5 oocytes) were −81±2 mV and 8.3±1.8 mV in control, and −81 mV±1 mV and 8.1±2.1 mV with genistein respectively. In Fig. 1F we plot the averaged time constants of activation (obtained by a fit to a single exponential relaxation) in control, and in the presence of genistein for five oocytes.

The calculated maximal whole-cell conductance tended to increase (+5.7±2.2%, n=5, n.s.) in the presence of genistein. Thus there appears to be little or no effect of genistein on the properties of HCN1.

Tyrosine kinase inhibition reduces HCN4-induced current and slows the kinetics of activation near $V_{1/2}$ without shifting the voltage dependence of activation

Figure 2 shows sample HCN4 induced membrane currents in control (Fig. 2A), in the presence of genistein (Fig. 2B) and after washout (Fig. 2C). The protocol was identical to that in Fig. 1 except that the duration of the first test pulse was 7.5 s, and that of the second step was 2 s. Figure 2D shows the step to −125 mV in control and in the presence of genistein. In contrast to HCN1-induced currents, there is a clear decrease in the amplitude of the HCN4-induced current at −125 mV in response to genistein. This decrease could be due to a decrease in channel conductance or a

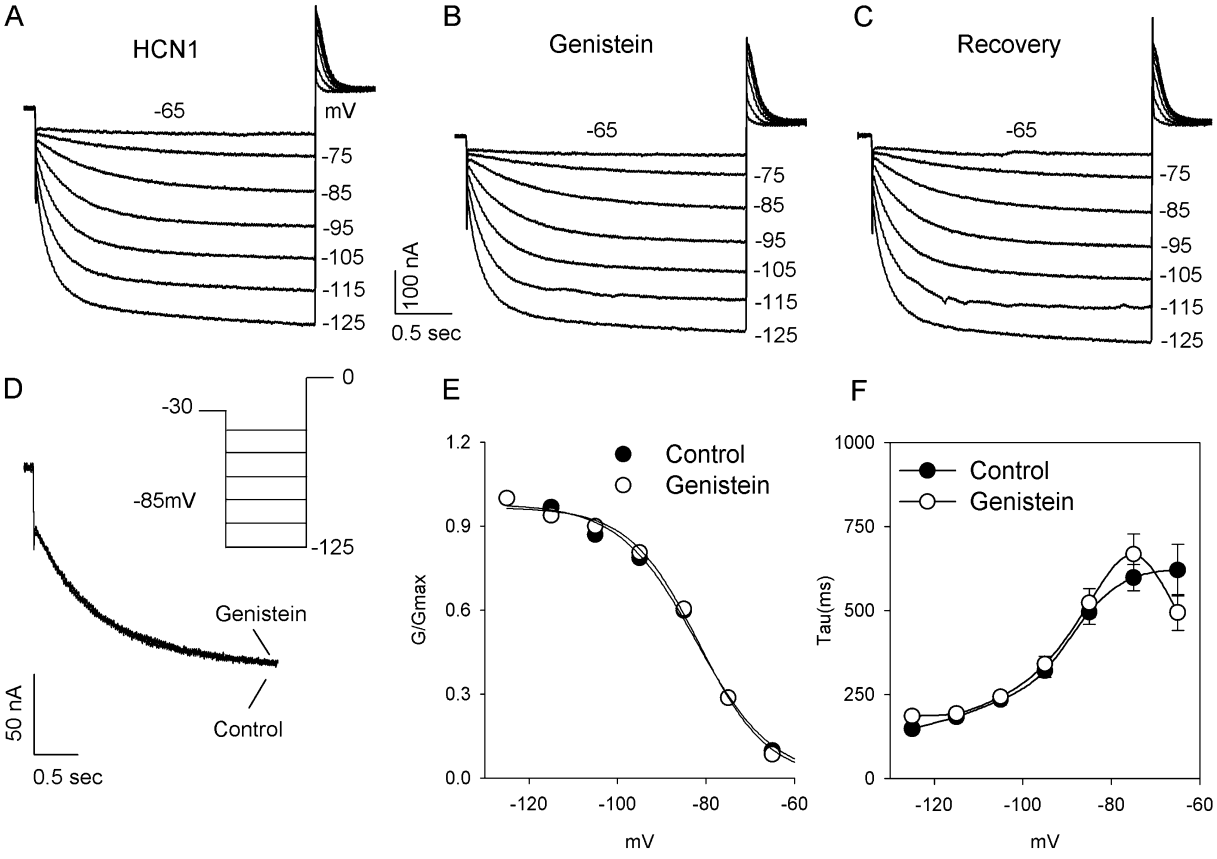

Fig.1A–F Genistein does not affect currents in *Xenopus* oocytes expressing hyperpolarization-activated, cyclic nucleotide-sensitive, non-selective cation channel-1 (HCN1). Currents were elicited by 2-s hyperpolarizing pulses between −65 mV and −125 mV. HCN1 current before (**A**), after perfusion with 0.1 mM genistein (**B**), and after washout of genistein (**C**). **D** At −85 mV, HCN1 currents in control and in the presence of genistein are plotted together and superimpose. The *inset* shows the pulse protocol used (see text for details). **E** Activation curves from the sample data shown in **A** and **B** for control (*solid circles*) and genistein (*open circles*). The *solid lines* show the fits to the Boltzmann equation. **F** Activation time constants (τ) in control and in the presence of genistein

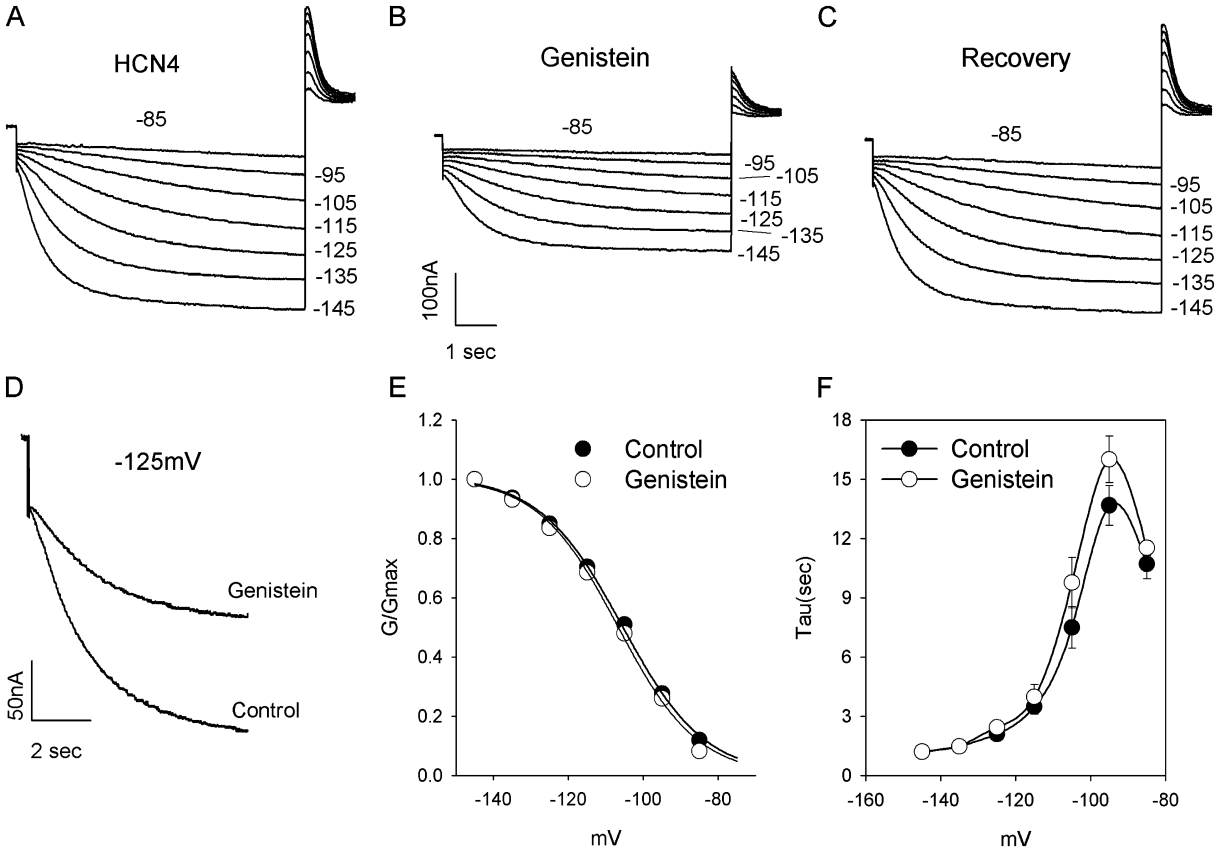

Fig. 2A–F Genistein inhibits HCN4 current. Currents were elicited by 7.5-s hyperpolarizing pulses between −85 mV and −145 mV. HCN4 current before (**A**), after perfusion with 0.1 mM genistein (**B**), and after washout of genistein (**C**) are shown. **D** Inhibition by genistein is shown by plotting HCN4 currents in control and in the presence of genistein at −125 mV. **E** Activation curves from the sample data shown in **A** and **B** for control (*solid circles*) and genistein (*open circles*). **F** Activation time constants in control and in the presence of genistein

negative shift in the voltage dependence of activation, or both.

Figure 2E shows the activation curves for the sample data shown in Fig. 2A and B. $V_{1/2}$ and s in this example are −106 mV and 11 mV in control and −107 mV and 11 mV in the presence of genistein respectively. The corresponding means (n=4 oocytes) are −105±2 mV and 10.2±1.3 mV in control and −105±2 mV and 9.1±1.1 mV in the presence of genistein respectively. Genistein did not change the midpoints or slopes significantly. The calculated maximal whole-cell conductance shows an average 46±13% (n=4, P<0.05) inhibition in response to genistein.

Figure 2F plots the averaged time constants of activation in control, and in the presence of genistein for four oocytes. The slowest rate of activation occurred near −95 mV in both solutions. At that voltage the time constant (τ_{max}) was larger in the presence of genistein than in control (control 14±1 s, genistein 16±1 s; P<0.05).

Taken as a whole, the results demonstrate that genistein inhibits the current by reducing the whole-cell conductance. This conductance effect is accompanied by a slowing of activation, without a concomitant shift in the voltage dependence of activation.

Tyrosine kinase inhibition reduces HCN2-induced currents, slows the kinetics of activation near $V_{1/2}$ and shifts the voltage dependence and kinetics of activation

Figure 3 shows sample HCN2-induced membrane currents in control (Fig. 3A), in the presence of genistein (Fig. 3B) and after washout (Fig. 3C). The protocol was identical to that in Fig. 2. Figure 3D shows the currents in response to the step to −95 mV in control and in the presence of genistein. There is a clear reduction in the amplitude of the current and a slowing of the kinetics of activation. These changes could be due to a reduction in conductance, and/or a shift in the voltage dependence of activation.

Figure 3E shows the activation curves for the sample data shown in Fig. 3A and B. $V_{1/2}$ and s in this example are −91 mV and 9.2 mV in control and −97 mV and 7.6 mV in the presence of genistein respectively. The corresponding means in (n=6 oocytes) are −93±3 mV and 7.6±0.5 mV for control, and −101±4 mV and 6.4±0.5mV in the presence of genistein respectively. The 8-mV shift in the presence of genistein is significant (P<0.05), while the 1.2-mV difference in slope is not. In parallel with the negative shift of $V_{1/2}$ for activation the threshold for activation of HCN2 was also more negative (about

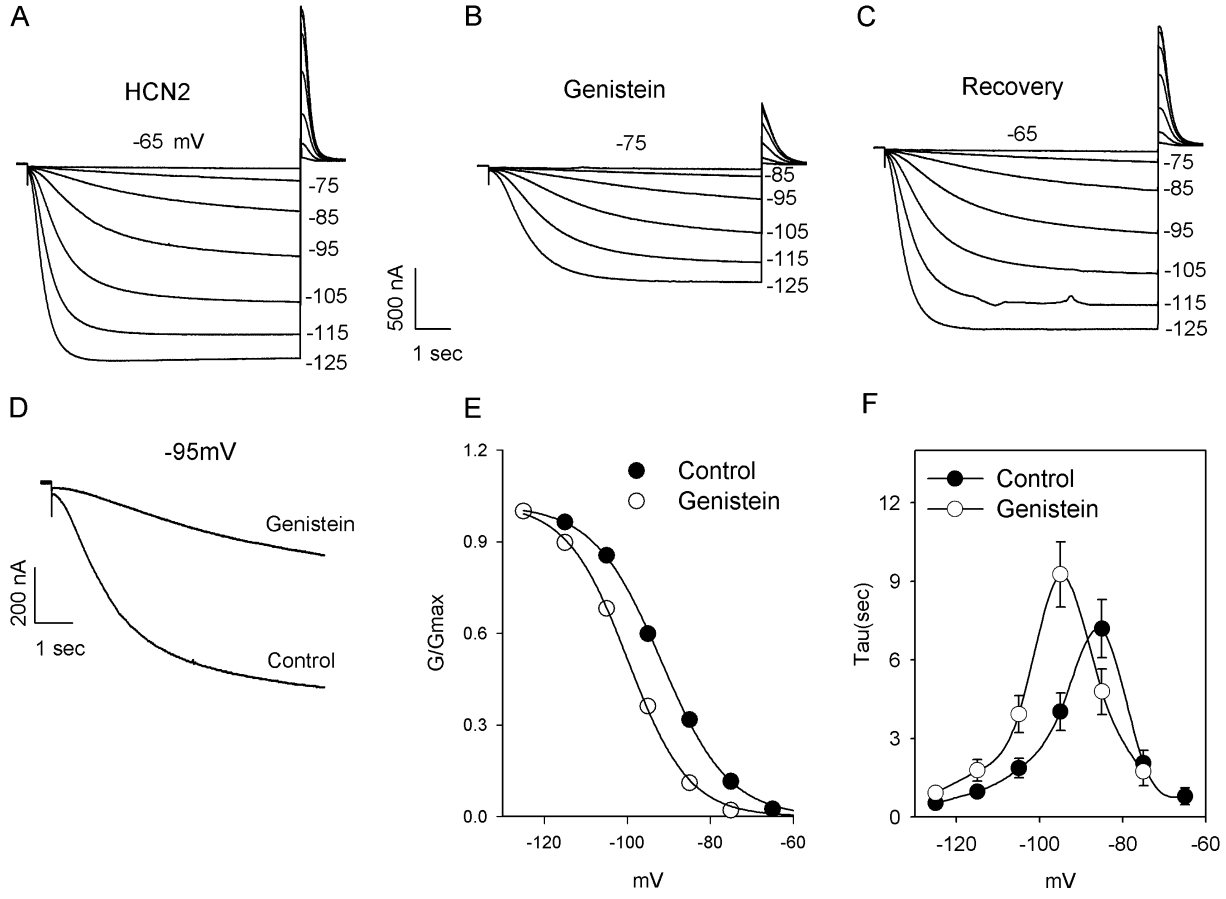

Fig. 3A–F Genistein inhibits HCN2 current. Currents were elicited by 7.5-s hyperpolarizing pulses between −65 mV and −125 mV. HCN2 current before (**A**), after perfusion with 0.1 mM genistein (**B**), and after washout of genistein (**C**) are shown. **D** Inhibition by genistein is shown by plotting HCN2 currents in control and in the presence of genistein at −95 mV. **E** Activation curves from the sample data shown in **A** and **B** for control (*solid circles*) and genistein (*open circles*). **F** Activation time constants in control and in the presence of genistein

−10 mV) with genistein than in control (Fig. 3A–C). Maximal whole-cell conductance is decreased (37±11%, n=5, P<0.05) by genistein.

Figure 3F plots the averaged time constants of activation in control and in the presence of genistein for five oocytes. Activation is slowest at −85 mV in control and at −95 mV in genistein. τ_{max} was 29±12% larger in the presence of genistein (P<0.05).

Taken as a whole these results demonstrate that genistein reduces the expressed current by reducing the whole-cell conductance and by shifting the voltage dependence of activation to more negative potentials. There is a similar shift in the kinetics of activation as well as an increase in the activation τ_{max}.

Daidzein, an inactive isomer of genistein, does not alter HCN2-induced currents

Previous studies employing genistein have shown that it sometimes reduces ion currents by blocking current flow through channels [7]. It seems unlikely that such an alternative existed in our case, since genistein had little or no effect on currents induced by open HCN1 channels, the pore of which is very similar to that of HCN2 or HCN4. Nevertheless a simple control experiment can evaluate such a possibility. Daidzein is an optical isomer of genistein with no effect on tyrosine kinases. Thus any reduction of HCN-induced currents by daidzein must occur through an alternative mechanism.

Figure 4 shows sample HCN2 currents in response to 4.5-s pulses in control solutions (Fig. 4A), in the presence of 100 μM daidzein (Fig. 4B) and after washout of daidzein (Fig. 4C). Figure 4D plots the HCN2-induced currents in response to the voltage step to −95 mV in control and in the presence of daidzein. The current is slightly larger in the presence of daidzein than in control.

Figure 4E shows the activation curve for the sample data for Fig. 4A and B. $V_{1/2}$ and s for this example are −95 mV and 10.1 mV for control and −96 mV and 10.9 mV respectively in the presence of daidzein. The corresponding means in (n=4 oocytes) are −97±2 mV and 9.8±2.5 mV in control and −97±2 mV and 10.1±2.4 mV for daidzein respectively. Neither $V_{1/2}$ nor s differed significantly from control in the presence of daidzein (P>0.05). The calculated maximal whole-cell conductance tended to increase by 13±11% (n=5, n.s.) in response to daidzein.

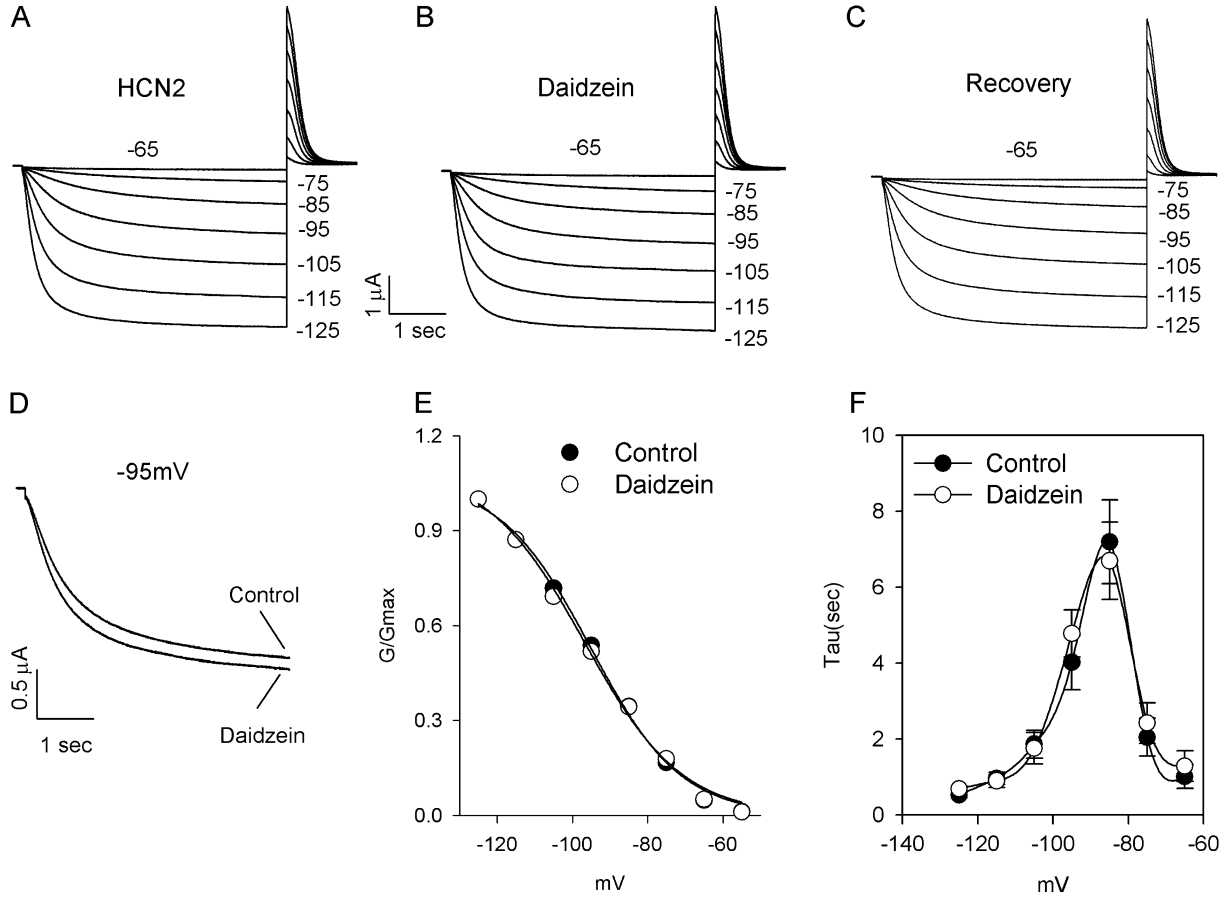

Fig. 4A–F Daidzein does not affect HCN2 current. Currents were elicited by 4.5-s hyperpolarizing pulses duration between −65 mV and −125 mV. HCN2 current before (**A**), after perfusion with 0.1 mM daidzein (**B**), and after washout of daidzein (**C**) are shown. **D** Plot of HCN2 currents in control and in the presence of daidzein at −95 mV showing slight increase of current in this cell in the presence of daidzein. **E** Activation curves from the sample data shown in **A** and **B** for control (*solid circles*) and daidzein (*open circles*). **F** Activation time constants in control and in the presence of daidzein

Figure 4F plots the averaged time constants of activation in control and in the presence of daidzein for four oocytes. The time constants in control did not differ from those in the presence of daidzein at any test potential.

These results suggest that daidzein has no effect on gating of HCN2 channels. Similar experiments were also performed on the expression of HCN1, and yielded the same lack of an effect of daidzein (data not shown). This further suggests that the actions of genistein on HCN2 and HCN4 are mediated by inhibition of tyrosine kinases.

Genistein reduces i_f in rat ventricular myocytes and shifts the voltage dependence and kinetics of activation

We have demonstrated previously that the rabbit SA node expresses HCN4 abundantly, with much less HCN2 and HCN1, while rabbit and rat ventricles express mainly HCN2 with much less HCN4 and no HCN1 [15]. The differential modulation by genistein of the three cardiac HCN isoforms predicts that genistein may reduce ventricular i_f and induce a negative shift in its voltage dependence and kinetics of activation.

We tested this hypothesis by examining genistein's actions on i_f in rat ventricular myocytes. We first examined the action of genistein on i_f density. Figure 5A shows that genistein reversibly inhibited i_f elicited by a 2-s hyperpolarizing step to −170 mV. Figure 5B summarizes results obtained from ten myocytes using this protocol. There was a more than threefold reduction in i_f induced by genistein which was partly reversible on washout (control: 12.2 ±1.8; genistein: 3.5±0.5; washout: 7.7±0.8 pA/pF). Figures 5C and D show currents in response to 3-s hyperpolarizing pulses from −100 mV to −180 mV in the presence and washout of genistein. Since with i_f rundown there is a negative shift in the voltage dependence of activation that could be confused with an action by genistein, we chose to compare results in the presence of genistein with those on washout. Any rundown would reduce the apparent effects of genistein on voltage dependence. The insets show changes in the threshold of i_f activation (V_{th}) from −110 mV (genistein) to −100 mV (washout) (V_{th} is −91±1 mV for control, −113±2 mV for genistein, and −98±2 mV for washout; n=7), demonstrating a negative shift of voltage dependence. We used i_f recorded at the test potentials and the measured reversal potential to construct the activation curves shown in

Fig. 5E (see figure legend). The Boltzmann two-state fit gave a 14-mV negative shift in voltage-dependent activation (genistein: $V_{1/2}$ −133±1 mV, s 8.5±0.9 mV; washout: $V_{1/2}$ −119±1 mV, *s* 9.1±1.0, both n=7). The difference in $V_{1/2}$ is significant (P<0.05). Figure 5F shows that the kinetics of activation shifted to more negative potentials in the presence of genistein (n=7) but without an apparent slowing.

Discussion

Our results demonstrate that genistein, an inhibitor of tyrosine kinases, has a differential action on heterologously expressed HCN currents in *Xenopus* oocytes. HCN1-induced current is insensitive to genistein while HCN2 and HCN4 induced currents are reduced. With expression of HCN4 the reduction in current amplitude is due to a voltage-independent decline in whole-oocyte

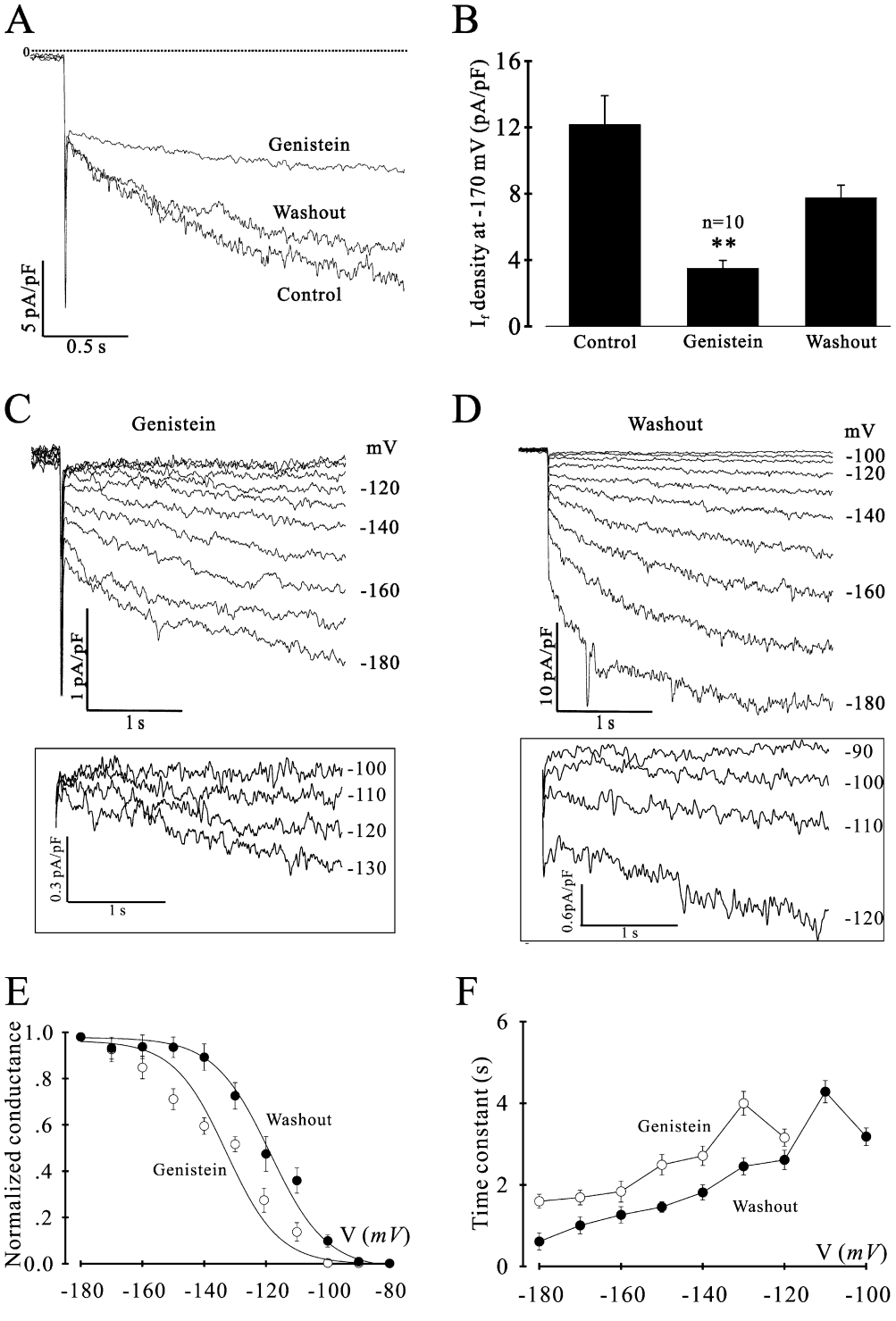

Fig. 5A–F Effect of genistein on i_f in rat ventricular myocytes. **A** Depression of i_f in representative rat ventricular myocytes by genistein and nearly complete reversal after washout. i_f was evoked by applying a 2 s hyperpolarizing voltage pulse to −170 mV from a holding potential of −50 mV. Currents are normalized to cell membrane capacitance. **B** Summary of the effect of genistein on i_f density in rat ventricular cells (n=10) P<0.05 vs. control. **C**, **D** Original traces of i_f activation in the presence of genistein (*upper panel* of **C**) and washout (*upper panel* of **D**) from a typical rat ventricular cell. i_f was activated by hyperpolarizing voltage steps from −80 mV to −180 mV (3 s duration) from a holding potential of −50 mV. Note the different *scale bars* for i_f density. In the same cell, current traces of i_f activation are displayed (shown at higher resolution) at voltages around its activation threshold in the presence of genistein (*lower panel* of **C**) and washout (*lower panel* of **D**). **E** Boltzmann fit (*solid lines*) of normalized ionic conductance for i_f showing that genistein (*open circles*) negatively shifted the potential of half-maximal activation compared with washout (*solid circles*). The activation curve was constructed by dividing the measured i_f at a given test voltage by the driving force where V_{rev} −4.0±0.6 mV (n=8) in 50 mM $[K^+]_o$. The currents were then normalized to the maximum current and fitted to the Boltzmann equation. **F** The mean time constants (τ) from a single exponential fit of i_f activation in the presence of genistein and washout in rat ventricular cells (n=7)

HCN conductance. However in the case of HCN2 there is a negative shift in the voltage dependence of activation that accompanies the decline in whole-cell conductance. Thus each HCN family member has its own unique response to tyrosine kinase inhibition.

Our previous studies of tyrosine phosphorylation state were executed in rabbit SA node myocytes [16, 17]. In this preparation inhibition of the kinase decreases whole-cell conductance, while an increase in tyrosine kinase activity induced by EGF increases whole-cell conductance. In neither study was the change in whole-cell conductance accompanied by a shift in the voltage dependence of activation. Given the results of the present study, this outcome is not surprising since more than 80% of HCN transcripts in rabbit sinus node is from the HCN4 message, with most of the remainder being HCN1 [15]. However, the reduction in conductance induced by genistein in the SA node is much smaller (about 23%) than that of HCN4 current induced by genistein (>45%, Fig. 2A, B). On the other hand, in the results presented above in rat ventricular myocytes the voltage dependence of activation of i_f is shifted in the negative direction by genistein. This is in agreement with genistein's effects on HCN2 expressed in oocytes. HCN2 is the major isoform in the rat ventricle [15]. However, the 8-mV negative shift induced by genistein in oocytes expressing HCN2 is significantly smaller than 14-mV shift of i_f induced by genistein in rat ventricular myocytes. Moreover, i_f current density is reduced nearly threefold in rat ventricular myocytes by genistein (Fig. 5B), a much larger effect than observed in oocytes at full activation (Figs. 3A, B). In addition, genistein slows both HCN2 and HCN4 kinetics of activation near the midpoint (Figs. 2F, 3F), but not those of i_f in ventricular myocytes (Fig. 5F). These differences in the magnitude of the inhibition and activation kinetics between oocytes and SA node or ventricular myocytes may be due to a number of alternatives including: (1) differences in the basal tyrosine phosphorylation of the channels, (2) the presence of heteromultimers, (3) the presence of different tyrosine kinases with different sensitivities to genistein, and/or (4) a difference in possible intermediary proteins or β-subunits that could modulate the action of genistein. Future investigations should help to decide among these alternatives.

We have no evidence at this point that genistein acts directly on the HCN channel subunits. Nevertheless it is worth pointing out that for all three HCN channels the NetPhos server (http://www.cbs.dtu.dk/services/NetPhos/, a web server that produces predictions for serine, threonine and tyrosine phosphorylation sites in eukaryotic proteins [1]) predicts there are specific intracellular tyrosine residues that, presumably, could be phosphorylated by tyrosine kinases (HCN1: Y400, Y406, Y547, Y657, Y708; HCN2: Y453, Y459, Y600, Y766; HCN4: Y531, Y537, Y678). The amino acid sequence in these sites are conserved among mouse [14], rat [9], rabbit [8], and human [10]. The roles that these tyrosine residues play in mediating the tyrosine phosphorylation of HCN isoforms will be further investigated.

There has been much interest in the development of non-beta-blocking bradycardic agents, and indeed blockers of i_f have been developed to fill this niche [2, 6]. However, i_f-like currents exist in other tissues including the photoreceptors of the eye, and disturbances of vision have been reported in about 30% of patients on which these "sinus-node inhibitors" have been employed [4]. The only HCN subunit expressed in photoreceptors is HCN1 [9], which is expressed at low levels only in the cardiac sinoatrial node. The two major isoforms in heart are HCN2 (ventricle) and HCN4 (SA node). Therefore, it is possible that a new generation of agents which reduce SA node i_f can now be developed based on the differential actions of tyrosine kinase inhibition on HCN isoforms as reported above.

Acknowledgements This work was supported by a Scientist Development Awards from American Heart Association to H. Yu, and by HL28958 and HL20558 from the National Heart, Lung, and Blood Institute to I. Cohen. We gratefully acknowledge the gift of HCN1 and HCN2 clones from Dr. B. Santoro and HCN4 clone from Dr. B. Kaupp.

References

1. Blom N, Gammeltoft S, Brunak S (1999) Sequence- and structure-based prediction of eukaryotic protein phosphorylation sites. J Mol Biol 294:1351–1362
2. BoSmith RE, Briggs I, Sturgess NC (1993) Inhibitory actions of Zeneca ZD7288 on whole-cell hyperpolarization activated inward current (I_f) in guinea-pig dissociated sinoatrial node cells. Br J Pharmacol 110:343–349
3. Davis MJ, Wu X, Nurkiewicz TR, Kawasaki J, Gui P, HILL MA, Wilson E (2001) Regulation of ion channels by protein tyrosine phosphorylation. Am J Physiol 281:H1835–H1862
4. Frishman WH, Pepine CJ, Weiss RJ, Baiker WM (1995) Addition of zatebradine, a direct sinus node inhibitor, provides no greater exercise tolerance benefit in patients with angina taking extended-release nifedipine: results of a multicenter, randomized, double-blind, placebo-controlled, parallel-group study. The Zatebradine Study Group. J Am Coll Cardiol 26:305–312
5. Gauss R, Seifert R, Kaupp UB (1998) Molecular identification of a hyperpolarization-activated channel in sea urchin sperm. Nature 393:583–587
6. Goethals M, Raes A, van Bogaert PP (1993) Use-dependent block of the pacemaker current i_f in rabbit sinoatrial node cells by zatebradine (UL-FS 49) on the mode of action of sinus node inhibitors. Circulation 88:2389–2401
7. Huang RQ, Dillon GH (2000) Direct inhibition of glycine receptors by genistein, a tyrosine kinase inhibitor. Neuropharmacology 39:2195–2204
8. Ishii TM, Takano M, Xie LH, Noma A, Ohmori H (1999) Molecular characterization of the hyperpolarization-activated cation channel in rabbit heart sinoatrial node. J Biol Chem 274:12835–12839
9. Jeon J, Strettoi E, Masland J (1998) The major cell populations of the mouse retina. J Neurosci 18:8936–8946
10. Ludwig A, Zong X, Jeglitsch M, Hofmann F, Biel M (1998) A family of hyperpolarization activated mammalian cation channels. Nature 393:587–591
11. Monteggia LM, Eisch AJ, Tang MD, Kaczmarek LK, Nestler EJ (2000) Cloning and localization of the hyperpolarization-activated cyclic nucleotide-gated channel family in rat brain. Mol Brain Res 81:129–139

12. Nair BG, Rashed HM, Patel TB (1993) Epidermal growth factor produces inotropic and chronotropic effects in rat hearts by increasing cyclic AMP accumulation, Growth Factors 8:41–48
13. Rabkin SW, Sunga P, Myrdal S (1987) The effect of epidermal growth factor on chronotropic response in cardiac cells in culture, Biochem Biophys Res Commun 146:889–897
14. Santoro B, Liu DT, Yao H, Bartsch D, Kandel ER, Siegelbaum SA, Tibbs GR (1998) Identification of a gene encoding a hyperpolarization activated pacemaker channel of brain. Cell 93:717–729
15. Shi W, Wymore R, Yu H, Wu J, Wymore RT, Pan Z, Robinson RB, Dixon JE, McKinnon D, Cohen IS (1999) Distribution and prevalence of hyperpolarization-activated cation channel (HCN) mRNA expression in cardiac tissues. Circ Res 85:e1–e6
16. Wu JY, Cohen IS (1997) Tyrosine kinase inhibition reduces i_f in rabbit SA myocytes. Pflugers Arch 434:509–514
17. Wu JY, Yu H, Cohen IS (2000) Epidermal growth factor increases i_f in rabbit SA node cells by activating a tyrosine kinase. Biochim Biophys Acta 1463:15–19
18. Yu H, Wu J, Potapova I, Wymore RT, Holmes B, Zuckerman J, Pan Z, Wang H, Shi W, Robinson R, El-Maghrabi MR, Benjamin W, Dixon J, McKinnon D, Cohen IS, Wymore R (2001) MinK-related peptide 1: a beta subunit for the HCN ion channel family, enhances expression and speeds kinetics. Circ Res 88:e84–e87